Eur. Phys. J. D **23**, 385–390 (2003)
DOI: 10.1140/epjd/e2003-00068-x

THE EUROPEAN PHYSICAL JOURNAL D

The He I 706.52 nm line shape characteristics in the plasma diagnostics

V. Milosavljević[a] and S. Djeniže

Faculty of Physics, University of Belgrade, P.O.B. 368, Belgrade, Serbia, Yugoslavia

Received 30 October 2002
Published online 15 April 2003 –

Abstract. On the basis of the precisely recorded 706.52 nm He I line shape we have obtained the basic plasma parameters *i.e.* electron temperature (T) and electron density (N) using our new line deconvolution procedure in the case of five various plasmas created in a linear, low–pressure, pulsed arc discharge. Plasma parameters have been also measured using independent experimental diagnostical techniques. Excellent agreement was found among the two sets of the obtained parameters. This enables our deconvolution procedure to recommendation for plasma diagnostical purposes, especially in astrophysics where direct measurements of the plasma parameters (T and N) are not possible. Besides, on the basis of the observed asymmetry of the Stark broadened line profile we have obtained its ion broadening parameter (A) caused by influence of the ion microfield to the line broadening mechanism and also the influence of the ion dynamic effect (D) to the line shape. Our A and D parameters represent the first data obtained experimentally using the line profile deconvolution procedure. We have found stronger influence of the ion contribution to the 706.52 nm He I line profile than the existing theoretical approximations estimate. This can be important for plasma modeling or for diagnostics.

PACS. 52.70.Kz Optical (ultraviolet, visible, infrared) measurements – 32.70.Jz Line shapes, widths, and shifts – 32.70.-n Intensities and shapes of atomic spectral lines

1 Introduction

Spectral line shapes represent important sources of information about the physical conditions in the place of birth of the radiation, especially since the launch of the Hubble space telescope. Many theoretical and experimental works have been devoted to the line shape investigations ([1–6] and references therein). Among them a significant number is dedicated to the neutral helium (He I) spectral lines. Namely, after hydrogen, helium is the most abundant element in the universe. Helium atoms and ions are present in many kinds of cosmic light sources and their radiation is very useful for astrophysical plasma diagnostical purposes. The 706.52 nm He I ($2p\ ^3\mathrm{P}^0_{2,1}$–$3s\ ^3\mathrm{S}_1$ transition) spectral line plays a special role. In the work [7] it is used to investigate the radiative transfer effects for a spherically symmetric nebula with no systematic velocity gradients. Izotov *et al.* [8] use this line to derive the ^{4}He abundance in the Metal-deficient Blue Compact Dwarf Galaxies Tol 1214-277 and Tol 65[1]. Recently, this line was used for various astrophysical investigations [9–12].

In this work we have applied our deconvolution procedure [13] to 706.52 nm He I line profile. On the basis of the precisely recorded 706.52 nm He I line shape we have obtained the basic plasma parameters *i.e.* electron temperature (T^{D}) and electron density (N^{D}) using our line deconvolution procedure in the case of five various plasmas created in linear, low–pressure, pulsed arc discharge in helium–nitrogen–oxygen mixture. To the knowledge of the authors, our results of the T and N values are the first published data obtained directly from the line deconvolution procedure. Plasma parameters have been also measured (T^{exp} and N^{exp}) using independent, well–known, experimental diagnostical techniques. Excellent agreement was found among the two sets of the obtained parameters (T^{D} and T^{exp}; and N^{D} and N^{exp}) enabling to recommend our deconvolution procedure for plasma diagnostical purposes, especially in astrophysics where direct measurements of the plasma parameters (T and N) are not possible.

In the plasmas with electron densities higher than 10^{21} m^{-3}, where the Stark effect plays an important role on the He I spectral lines broadening, the Stark broadening characteristics can be used for plasma diagnostical purposes, also. A significant number of theoretical and experimental works are devoted to the He I Stark FWHM (full-width at half intensity maximum, W) investigations. However, only three experiments [14–16] deal with the determination of the total Stark width (electron + ion) of the He I 706.52 nm line and four works [2,17–19] contain

[a] e-mail: vladimir@ff.bg.ac.yu

theoretical calculations devoted to this field. In this work we will present measured Stark broadening parameters of the 706.52 nm He I spectral line at (18 000–33 000) K electron temperatures and at (4.4–8.2)$\times 10^{22}$ m^{-3} electron densities. Using a deconvolution procedure described in [13] and already applied in the case of some He I and Ne I lines [20–22] we have obtained, for the first time, on the basis of the observed line profile asymmetry, the characteristics of the ion contribution to the total Stark FWHM (W_t) expressed in term of the ion contribution parameter (A) and ion–dynamic effect (D) [2,17,23] and, also, the separate electron (W_e) and ion (W_i) contribution to the total Stark width (W_t) of the 706.52 nm He I spectral line. As an optically thin plasma source we have used the linear, low-pressure, pulsed arc operated in five various discharge conditions. Our W_t, W_e, W_i and A values have been compared to all available theoretical and experimental Stark broadening parameters.

2 Theoretical background

The total line Stark FWHM (W_t) is given as

$$W_\mathrm{t} = W_\mathrm{e} + W_\mathrm{i}, \tag{1}$$

where W_e and W_i are the electron and ion contributions, respectively. For a non–hydrogenic, isolated neutral atom line the ion broadening is not negligible and the line profiles are described by an asymmetric K function (see Eq. (6) in Sect. 3 and in [13]). The total Stark width (W_t) may be calculated from the equation [2,15,23]:

$$W_\mathrm{t} \approx W_\mathrm{e}[1 + 1.75AD(1 - 0.75R)], \tag{2}$$

where

$$R = \sqrt[6]{\frac{36\pi e^6 N}{(kT)^3}}, \tag{3}$$

is the ratio of the mean ion separation to the Debye length. N and T represent electron density and temperature, respectively. A is the quasi–static ion broadening parameter (see Eq. (224) in [2]) and D is a coefficient of the ion-dynamic contribution with the established criterion:

$$D = \frac{1.36}{1.75(1 - 0.75R)} B^{-1/3} \quad \text{for} \quad B < \left(\frac{1.36}{1.75(1 - 0.75R)}\right)^3;$$

or

$$D = 1 \quad \text{for} \quad B \geq \left(\frac{1.36}{1.75(1 - 0.75R)}\right)^3, \tag{4}$$

where

$$B = A^{1/3} \frac{4.03 \times 10^{-7} W_\mathrm{e}[\mathrm{nm}]}{(\lambda[\mathrm{nm}])^2} (\mathrm{N}[\mathrm{m}^{-3}])^{2/3} \sqrt{\frac{\mu}{T_\mathrm{g}[\mathrm{K}]}} < 1; \tag{5}$$

is the factor with atom-ion perturber reduced mass μ (in amu) and gas temperature T_g. When $D = 1$ the influence of the ion–dynamic is negligible and the line shape is treated using the quasi–static ion approximation. From equations (1–6) it is possible to obtain the plasma parameters (N and T) and the line broadening characteristics (W_t, W_e, W_i, A and D). One can see that the ion contribution, expressed in terms of the A and D parameters directly determine the ion width (W_i) component in the total Stark width (Eqs. (1, 2)).

3 Numerical procedure for deconvolution

The proposed functions for various line shapes, equation (6) is of the integral form and include several parameters. Some of these parameters can be determined in separate experiments, but not all of them. Furthermore, it is impossible to find an analytical solution for the integrals and methods of numerical integration have to be applied. This procedure, combined with the simultaneous fitting of several free parameters, causes the deconvolution to be an extremely difficult task and requires a number of computer supported mathematical techniques. Particular problems are the questions of convergence and reliability of the deconvolution procedure, which are tightly connected with the quality of experimental data

$$K(\lambda) = K_\mathrm{o} + K_\mathrm{max} \int_{-\infty}^{\infty} \exp(-t^2) \times \left[\int_0^{\infty} \frac{H_\mathrm{R}(\beta)}{1 + \left(2\frac{\lambda - \lambda_\mathrm{o} - \frac{W_\mathrm{G}}{2\sqrt{\ln 2}} t}{W_\mathrm{e}} - \alpha\beta^2\right)^2} \mathrm{d}\beta \right] \mathrm{d}t. \tag{6}$$

Here K_o is the baseline (offset) and K_max is the maximum of intensity (intensity for $\lambda = \lambda_\mathrm{o}$) [13]. $H_\mathrm{R}(\beta)$ is an electric microfield strength distribution function of normalized field strength $\beta = F/F_\mathrm{o}$, where F_o is the Holtsmark field strength. A ($\alpha = A^{4/3}$) is the static ion broadening parameter and is a measure of the relative importance of ion and electron broadenings. R is the ratio of the mean distance between the ions to the Debye radius (see Eq. (3)), *i.e.* the Debye shielding parameter and W_e is the electron width (FWHM) in the $j_\mathrm{A,R}$ profile [2].

For the purpose of deconvolution iteration process we need to know the value of K (Eq. (6)) as a function of λ for every group of parameters (K_max, λ_o, W_e, W_G, R, A). W_G is defined in equation (2.3) in [13]. The used numerical procedure for the solution of equation (6) is described in earlier publications [13,20,24]. It should be noted that application of a deconvolution and fitting method requires some assumptions or prior knowledge about plasma condition. Accordingly, for each emitter ionization stage one needs to know the electric microfield distribution, in order to fit the K functions. In the cases of quasi–static or quasi–static and dynamic broadening, our fitting procedure gives the electron impact width (W_e), static ion

Table 1. Various discharge conditions. C-bank capacity (in μF), U-bank voltage (in kV), H-plasma length (in cm), Φ-tube diameter (in mm), P-filling pressure (in Pa). $N^{\rm exp}$ (in 10^{22} m^{-3}) and $T^{\rm exp}$ (in 10^3 K) denote measured electron density and temperature values, respectively obtained at a 25th μs after the beginning of the discharge when the line profiles were analyzed. $N^{\rm D}$ (in 10^{22} m^{-3}) and $T^{\rm D}$ (in 10^3 K) are values obtained using line deconvolution procedure at a 25th μs.

Exp.	C	U	H	Φ	P	$N^{\rm exp}$	$N^{\rm D}$	$T^{\rm exp}$	$T^{\rm D}$
a	8	4.5	6.2	5	267	6.1	5.4	33.0	31.4
b_1	14	4.2	14.0	25	267	8.2	7.5	31.5	30.5
b_2	14	3.4	14.0	25	267	6.7	6.9	30.0	30.2
b_3	14	2.6	14.0	25	267	4.4	4.0	28.0	27.1
b_4	14	1.5	7.2	5	133	5.0	4.9	18.0	17.6

broadening parameter (A) and, finally dynamic ion broadening parameter (D).

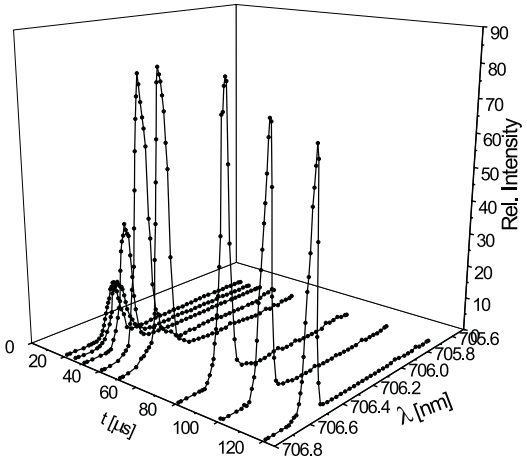

Fig. 1. Temporal evolution of the 706.52 nm He I line profile recorded under discharge conditions $C = 14$ μF and $U = 1.5$ kV (see Tab. 1).

4 Experiment

The modified version of the linear low–pressure pulsed arc [20–22,24–27] has been used as a plasma source. A pulsed discharge was driven in a quartz discharge tube at different inner diameters and plasma lengths. Various dimensions of the discharge tube offer the possibility of the electron temperature variation in a wide range. The working gas was helium–nitrogen–oxygen mixture (90% He + 8% N_2 + 2% O_2). The used tube geometry and corresponding discharge conditions are presented in Table 1.

Spectroscopic observation of spectral lines was made end-on along the axis of the discharge tube.

The line profiles were recorded by a step-by-step technique using a photomultiplier (EMI 9789 QB and EMI 9659B) and a grating spectrograph (Zeiss PGS-2, reciprocal linear dispersion 0.73 nm/mm in the first order) system. The instrumental FWHM of 8 pm was obtained by using narrow spectral lines emitted by the hollow cathode discharge. The spectrograph exit slit (10 μm) with the calibrated photomultipliers was micrometrically traversed along the spectral plane in small wavelength steps (7.3 pm). The averaged photomultiplier signal (five shots in each position) was digitized using an oscilloscope, interfaced to a computer. A sample output, as an example, is shown in Figure 1.

Plasma reproducibility was monitored by the He I (501.5 nm, 388.8 nm and 587.6 nm) lines radiation and, also, by the discharge current using Rogowski coil signal (it was found to be within ±5%).

The used deconvolution procedure in its details is described in [13,24] and, briefly in Section 3. It includes a new advanced numerical procedure for deconvolution of theoretical asymmetric convolution integral of a Gaussian and a plasma broadened spectral line profile $j_{\rm A,R}(\lambda)$ for spectral lines. This method gives complete information on the plasma parameters from a single recorded spectral line. The method determines all broadening ($W_{\rm t}$, $W_{\rm e}$, $W_{\rm i}$, A and D) and plasma parameters (N and T) self–consistently and directly from the shape of spectral lines without any assumptions (see Sect. 3) making it useful in astrophysics. The measured profiles were convoluted due to the convolutions of the Lorentzian Stark and Gaussian profiles caused by Doppler and instrumental broadenings [2]. Van der Waals and resonance broadenings [2] were estimated to be smaller by more than an order of magnitude in comparison to Stark, Doppler and instrumental broadenings. The deconvolution procedure was computed using the least Chi-square function (see Sect. 3).

The plasma parameters were determined using standard diagnostics methods. Thus, the electron temperature was determined from the ratios of the relative line intensities of four N III spectral lines (409.74 nm, 410.34 nm, 463.42 nm and 464.06 nm) to the 463.05 nm N II spectral line with an estimated error of ±10 %, assuming the existence of the LTE [2]. All the necessary atomic data have been taken from [6,28]. The electron density decay was measured using a well-known single wavelength He–Ne laser interferometer technique for the 632.8 nm transition with an estimated error of ±9%. The experimental electron densities ($N^{\rm exp}$) and temperatures ($T^{\rm exp}$), obtained at the moment when the line profiles were analyzed, are presented in Table 1 together with the $N^{\rm D}$ and $T^{\rm D}$ values obtained from deconvolution procedures. Temporal evolution of electron temperatures ($T^{\rm exp}$ and $T^{\rm D}$) and electron densities ($N^{\rm exp}$ and $N^{\rm D}$) are presented in Figure 2.

5 Results and discussion

The measured $N^{\rm exp}$ and $T^{\rm exp}$ decays are presented in Figure 2 together with the $N^{\rm D}$ and $T^{\rm D}$ values obtained using the line profile deconvolution procedure for the 706.52 nm He I line. One can conclude that the agreement among $N^{\rm exp}$ and $N^{\rm D}$ values is excellent (within 4% on average in the investigated five plasmas). This fact confirms the homogeneity of plasmas in the linear part of our light source

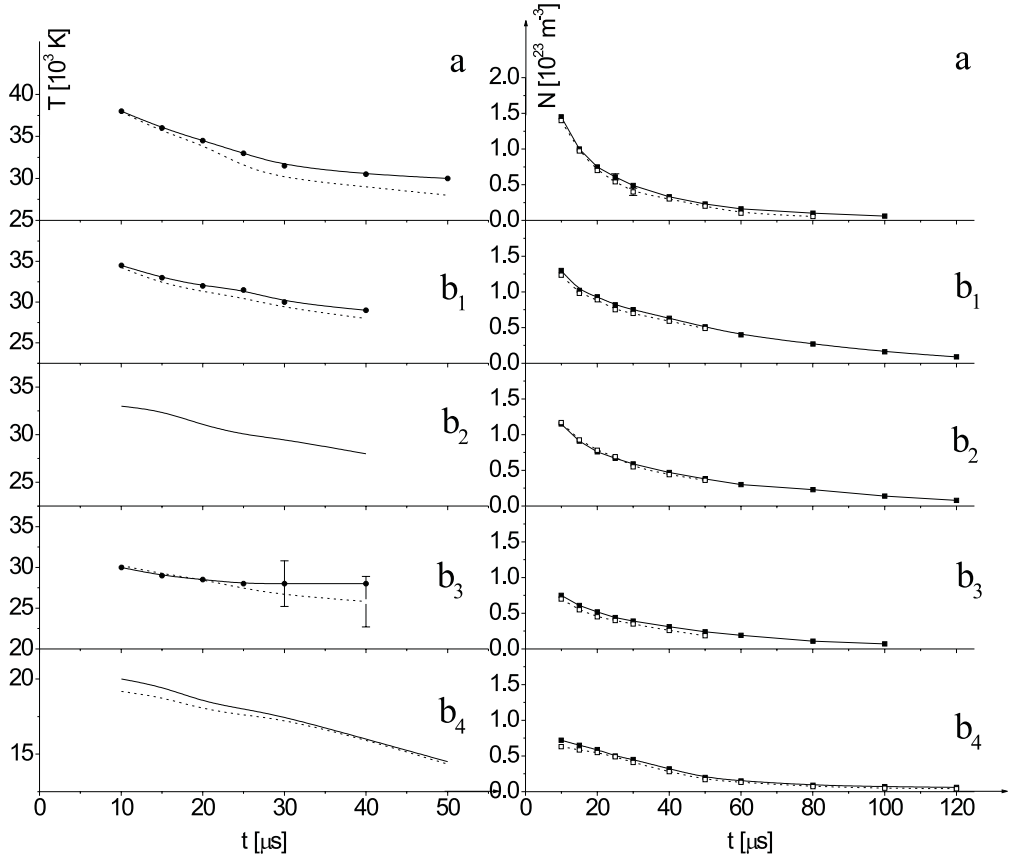

Fig. 2. Electron temperature (T) and density (N) decays. Full lines represent measured data using independent experimental techniques and dashed lines represent plasma parameters obtained using our line deconvolution procedure in various plasmas (see Tab. 1). Error bars, indicated only in the case of the greatest disagreement (T in b_3), represent estimated accuracies of the measurements (±10%) and deconvolutions (±12%).

(Fig. 1 in [26]). In the case of the electron temperature the situation is similar but the agreement among the two sets of the electron temperature decays is poorer. This can be explained taking into account the nature of the applied method of the measurement of the electron temperature. Namely, it should be remarked that the uncertainty of the used experimental method (Saha equation) depends on the existence of the LTE during the plasma decay. Existence of the LTE is estimated in the phases of the plasma decay when the electron concentration fulfills the criterion of the existence of the LTE [2,3]. In our experiment N II and N III energy level (used in the Saha equation) populations remain in the LTE up to 50 μs after the beginning of the discharge (in all experiments). After this moment the Saha equation gives unreliable results. Within the experimental accuracy (±10%) of the electron temperature measurements and the uncertainties (±12%) of the T^{D} values obtained using the line deconvolution procedure, the T^{exp} and T^{D} values agree up to 50 μs after the beginning of the discharge confirming our estimations about the existence of the LTE. This statement also confirm the homogeneity of the created plasmas.

Plasma broadening parameters (W_{t}, W_{e}, W_{i}, A, D) obtained by our deconvolution procedure of the recorded line profiles at measured N and T values are presented in Table 2 together with other authors ones. Various theoretical (G, BCW, DSB) predictions of the W_{e}, W_{i} and A are also given. By the normalization of the A^{G} and A^{BCW} values to our electron density the well–known $N^{1/4}$ numerical factor [2] was used.

In order to make the comparison among measured ($W_{\mathrm{t}}^{\mathrm{exp}}$) and calculated ($W_{\mathrm{t}}^{\mathrm{th}}$) total (electron + ion) width values easier the ratio $W_{\mathrm{t}}^{\mathrm{exp}}/W_{\mathrm{t}}^{\mathrm{th}}$ dependence on the electron temperature are presented graphically in Figure 3. The $W_{\mathrm{t}}^{\mathrm{G}}$ [2] and $W_{\mathrm{t}}^{\mathrm{BCW}}$ [17] values are calculated using equation (226) from [2] with the W_{e} and A values predicted by the G [2] and BCW [17] theoretical approaches, respectively. The $W_{\mathrm{t}}^{\mathrm{exp}}/W_{\mathrm{t}}^{\mathrm{th}}$ ratios related to the [19] data have been calculated only for our experimental values. Namely, for the $W_{\mathrm{i}}^{\mathrm{DSB}}$ calculations it is necessary to know the helium ion concentration connected to the plasma composition. We have performed this for our discharge conditions only.

Our broadening parameter ($W_{\mathrm{t}}^{\mathrm{exp}}$) represent the first measured value at electron densities higher than 10^{22} m^{-3}. It turns out that our $W_{\mathrm{e}}^{\mathrm{exp}}$ and $W_{\mathrm{i}}^{\mathrm{exp}}$ are the first separated experimental electron and ion Stark width data, obtained using our deconvolution procedure. They are

Table 2. Line broadening characteristics. Measured: total Stark FWHM (W_t^{exp} in pm within ±12% accuracy), electron and ion (He^+) Stark widths (W_e^{exp} and W_i^{exp} in pm within ±12% accuracy), quasistatic ion broadening parameter (A^{exp}, dimensionless within ±15% accuracy) and ion dynamic coefficient (D^{exp}, dimensionless within ±20% accuracy) at measured electron temperatures (T^{exp} in 10^3 K) and electron densities (N^{exp} in 10^{22} m^{-3}). Ref. presents Tw, K, M and MS values given in this work (Tw) and those used from Kelleher [15], Mijatović *et al.* [16] and Mazing and Slemzin [14], respectively. Asterisk denote first experimental values [15]. The index G, BCW and DSB denote theoretical data taken from Griem [2]; Bassalo *et al.* [17] and Dimitrijević and Sahal-Bréchot [19], respectively at a given T and N.

T^{exp}	N^{exp}	W_t^{exp}	W_e^{exp}	W_i^{exp}	A^{exp}	D^{exp}	Ref.	W_e^G	W_e^{BCW}	W_e^{DSB}	W_i^{DSB}	A^G	A^{BCW}
33.0	6.1	281	234	47	0.148	1.51	Tw	307	273	224	46	0.082	0.089
31.5	8.2	372	307	65	0.160	1.42	Tw	411	361	298	58	0.089	0.099
30.0	6.7	300	250	50	0.152	1.49	Tw	333	292	241	51	0.085	0.094
28.0	4.4	190	161	29	0.136	1.65	Tw	217	190	156	29	0.077	0.085
18.0	5.0	211	179	32	0.145	1.62	Tw	232	203	171	26	0.083	0.092
20.9	1.03	47			0.031*	2.33*	K						
21.4	0.34	17					M						
22.7	0.45	22					M						
23.6	0.59	29					M						
34.8	1.0	51					MS						

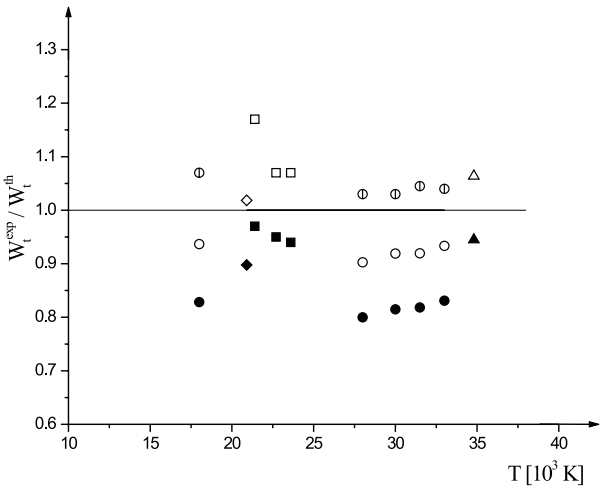

Fig. 3. Ratios of the experimental total Stark FWHM (W_t^{exp}) to the various theoretical (W_t^{th}) predictions *vs.* electron temperature. Circle, diamond, triangle and square represent our experimental data and those from Kelleher [15], Mazing and Slemzin [14] and Mijatović *et al.* [16], respectively. Filled, empty and half divided symbols represent the ratios related to the theories taken from Griem [2], Bassalo *et al.* [17] and Dimitrijević and Sahal–Bréchot [19], respectively.

in excellent agreement (within ±4%) with W_e^{DSB} and (within ±8%) with W_i^{DSB} [19] values. Theoretical W_e^G [2] and W_e^{BCW} [17] values are higher than ours by about 33% and 17% (on average), respectively. By the inspection of the Figure 3 one can conclude that Griem's total half-widths lie above all other experimental and theoretical values. Experimental total half–widths, including ours, agree well (within ± 10%) with calculated values from [17]. Our W_t^{exp} are in excellent agreement with W_t^{DSB} form [19] (see Fig. 3). It turns out that our W_i^{exp}/W_t^{exp} (16% on average) are in excellent agreement with W_i^{DSB}/W_t^{DSB} (also 16% on average) theoretical values [19]. We found evident contribution of the ion influence to the line broadening due to the quasi–static ion and ion–dynamic effects. The quasi–static ion effect is higher than the G [2] and BCW [17] approaches estimate by about 70% and 50%, respectively. Besides, we have also found that the ion–dynamic effect plays an important role. This effect multiplies the quasi–static ion influence about 1.5 times at our plasma parameters and composition and show increasing tendency at lower electron densities confirming the theoretical [2,23] estimations.

6 Conclusion

Using line deconvolution procedure [13,24] we have obtained, on the basis of the precisely recorded He I 706.52 nm spectral line profile its Stark broadening parameters: W_t, W_e, W_i, A and D and the main plasma parameters (N and T). We have found that the ion contribution to the line profile plays a more important role than the semiclassical [2,17] theoretical approximations estimate, and that must be taken into account for the use of the He I 706.52 nm line for plasma diagnostical purposes. Similar behaviors have been predicted by the semiclassical perturbation formalism [19].

This work is a part of the project "Determination of the atomic parameters on the basis of the spectral line profiles" supported by the Ministry of Science, Technologies and Development of the Republic of Serbia.

References

1. H.R. Griem, *Plasma Spectroscopy* (McGraw-Hill Book Company, New York, 1964)
2. H.R. Griem, *Spectral Line Broadening by Plasmas* (Acad. Press, New York, 1974)

3. H.R. Griem, *Principles of Plasma Spectroscopy* (Univ. Press, Cambridge, 1997)
4. A. Lesage, J.R. Fuhr, *Bibliography on Atomic Line Shapes and Shifts (April 1992 through June 1999)* (Observatoire de Paris, 1999)
5. N. Konjević, A. Lesage, J.R. Fuhr, W.L. Wiese, J. Phys. Chem. Ref. Data **31**(3), 819 (2002)
6. NIST - Atomic Spectra Data Base Lines (wavelength order) – `http://physics.nist.gov` (2002)
7. R.A. Benjamin, E.D. Skillman, D.S. Smits, Astrophys. J. **569**, 288 (2002)
8. Y.I. Izotov, F.H. Chaffee, R.F. Green, Astrophys. J. **562**, 727 (2001)
9. D. Branch *et al.*, Astrophys. J. **566**, 1005 (2002)
10. C. Fransson *et al.*, Astrophys. J. **572**, 350 (2002)
11. R. Vázquez *et al.*, Astrophys. J. **576**, 860 (2002)
12. N.A. Webb, T. Naylor, R.D. Jeffries, Astrophys. J. **568**, L45 (2002)
13. V. Milosavljević, G. Poparić, Phys. Rev. E **63**, 036404 (2001)
14. M.A. Mazing, V.A. Slemzin, Sov. Phys. Lebedev Inst. Rep. **4**, 42 (1973)
15. D.E. Kelleher, JQSRT **25**, 191 (1981)
16. Z. Mijatović, N. Konjević, M. Ivković, R. Kobilarov, Phys. Rev. E **51**, 4891 (1995)
17. J.M. Bassalo, M. Cattani, V.S. Walder, JQSRT **28**, 75 (1982)
18. M.S. Dimitrijević, S. Sahal−Bréchot, JQSRT **31**, 301 (1984)
19. M.S. Dimitrijević, S. Sahal−Bréchot, A&A Supp. Ser. **82**, 519 (1990)
20. V. Milosavljević, S. Djeniže, A&A **393**, 721 (2002)
21. V. Milosavljević, S. Djeniže, New Astron. **7/8**, 543 (2002)
22. V. Milosavljević, S. Djeniže, Phys. Lett. A **305/1-2**, 70 (2002)
23. A.J. Barnard, J. Cooper, E.W. Smith, JQSRT **14**, 1025 (1974)
24. V. Milosavljević, Ph.D. thesis, University of Belgrade, Faculty of Physics, Belgrade, 2001
25. V. Milosavljević, S. Djeniže, Eur. Phys. J. D **15**, 99 (2001)
26. S. Djeniže, V. Milosavljević, A. Srećković, JQSRT **59**, 71 (1998)
27. S. Djeniže, A. Srećković, S. Bukvić, Eur. Phys. J. D **20**, 11 (2002)
28. S. Glenzer, H. J. Kunze, J. Musielok, Y. Kim, W.L. Wiese, Phys. Rev. A **49**, 221 (1994)